Original Article | Oncologic Imaging

eISSN 2005-8330
https://doi.org/10.3348/kjr.2023.0618
Korean J Radiol 2024;25(2):189-198

Korean Journal of Radiology
KJR

Prognostic Value of ^{18}F-FDG PET/CT Radiomics in Extranodal Nasal-Type NK/T Cell Lymphoma

Yu Luo[1,2], Zhun Huang[1], Zihan Gao[1], Bingbing Wang[1], Yanwei Zhang[3], Yan Bai[1], Qingxia Wu[4], Meiyun Wang[1,5,6]

[1]Department of Medical Imaging, Henan Provincial People's Hospital, The People's Hospital of Zhengzhou University, Zhengzhou, China
[2]Academy of Medical Sciences, Zhengzhou University, Zhengzhou, China
[3]Department of Bethune International Peace Hospital, Department of Radiology, Shijiazhuang, China
[4]Beijing United Imaging Research Institute of Intelligent Imaging, Beijing, China
[5]Henan Key Laboratory for Medical Imaging of Neurological Diseases, Zhengzhou, China
[6]Laboratory of Brain Science and Brain-Like Intelligence Technology, Institute for Integrated Medical Science and Engineering, Henan Academy of Sciences, Zhengzhou, China

Objective: To investigate the prognostic utility of radiomics features extracted from ^{18}F-fluorodeoxyglucose (FDG) PET/CT combined with clinical factors and metabolic parameters in predicting progression-free survival (PFS) and overall survival (OS) in individuals diagnosed with extranodal nasal-type NK/T cell lymphoma (ENKTCL).

Materials and Methods: A total of 126 adults with ENKTCL who underwent ^{18}F-FDG PET/CT examination before treatment were retrospectively included and randomly divided into training (n = 88) and validation cohorts (n = 38) at a ratio of 7:3. Least absolute shrinkage and selection operation Cox regression analysis was used to select the best radiomics features and calculate each patient's radiomics scores (RadPFS and RadOS). Kaplan–Meier curve and Log-rank test were used to compare survival between patient groups risk-stratified by the radiomics scores. Various models to predict PFS and OS were constructed, including clinical, metabolic, clinical + metabolic, and clinical + metabolic + radiomics models. The discriminative ability of each model was evaluated using Harrell's C index. The performance of each model in predicting PFS and OS for 1-, 3-, and 5-years was evaluated using the time-dependent receiver operating characteristic (ROC) curve.

Results: Kaplan–Meier curve analysis demonstrated that the radiomics scores effectively identified high- and low-risk patients (all $P < 0.05$). Multivariable Cox analysis showed that the Ann Arbor stage, maximum standardized uptake value (SUVmax), and RadPFS were independent risk factors associated with PFS. Further, β2-microglobulin, Eastern Cooperative Oncology Group performance status score, SUVmax, and RadOS were independent risk factors for OS. The clinical + metabolic + radiomics model exhibited the greatest discriminative ability for both PFS (Harrell's C-index: 0.805 in the validation cohort) and OS (Harrell's C-index: 0.833 in the validation cohort). The time-dependent ROC analysis indicated that the clinical + metabolic + radiomics model had the best predictive performance.

Conclusion: The PET/CT-based clinical + metabolic + radiomics model can enhance prognostication among patients with ENKTCL and may be a non-invasive and efficient risk stratification tool for clinical practice.

Keywords: Extranodal nasal-type NK/T-cell lymphoma; PET/CT; Radiomics; Prognosis; Nomogram

INTRODUCTION

Extranodal nasal-type NK/T cell lymphoma (ENKTCL) is a subtype of non-Hodgkin lymphoma that occurs outside lymph nodes and is characterized by special morphology, immunophenotype, and biological behavior [1]. ENKTCL exhibits high malignancy, invasiveness, and rapid progression [2]. Currently, no standard treatment

Received: June 30, 2023 **Revised:** November 8, 2023 **Accepted:** November 16, 2023
Corresponding author: Meiyun Wang, MD, PhD, Department of Medical Imaging, Henan Provincial People's Hospital, No. 7 Weiwu Road, Jinshui District, Zhengzhou 450003, China
• E-mail: mywang@zzu.edu.cn

regimen exists for ENKTCL. Due to drug-resistance genes and overexpression of P-glycoprotein in tumor cells, the L-asparaginase-based chemotherapy regimen is widely used in clinical practice [3]. While combined chemoradiotherapy has been shown to achieve a 5-year overall survival (OS) rate of up to 59% in patients, some still exhibit recurrence and resistance [4,5]. Therefore, early identification of high-risk patients with a propensity for progression or recurrence is critical for individualized precision therapy, clinical treatment decision-making, and accurate prognostic prediction.

^{18}F-fluorodeoxyglucose (^{18}F-FDG) PET/CT is a whole-body imaging technique that combines functional metabolism and anatomical structure [6]. It provides detailed information—including lesion size, location, metabolic activity, and metastasis—valuable in diagnosing and treating patients. Previous studies have shown that semi-quantitative parameters—including maximum standardized uptake value (SUVmax), metabolic tumor volume (MTV), and total lesion glycolysis (TLG)—may serve as reliable prognostic indicators for patients with ENKTCL [7-9]. However, ENKTCL can induce chronic inflammation in the nasal cavity and nasopharynx, which may impact the accuracy of measurements. Furthermore, the above parameters are obtained from setting corresponding thresholds for delineated regions of interest, which may not fully capture the spatial distribution characteristics of tracer activity strongly associated with tumor heterogeneity [10,11]. Radiomics offers potential pathophysiological information through high-throughput extraction of features from medical images, quantitatively analyzes tumor heterogeneity, and selects features for constructing prognostic prediction models through specific algorithms and statistical analysis to promote the development of precise and individualized tumor treatment [12,13]. Tumor heterogeneity is a key factor in determining disease aggressiveness and is closely related to proliferation, differentiation, and metabolism [14]. Radiomics overcomes the limitations of clinical dependence on the subjective experience of diagnostic physicians and significantly expands the guiding value of medical imaging in clinical practice. While PET/CT radiomics has been applied to various malignant tumors, few studies exist on ENKTCL [15-17]. Therefore, this study aimed to explore the prognostic efficacy of PET/CT radiomics features combined with clinical risk factors and tumor metabolic load in patients with ENKTCL.

MATERIALS AND METHODS

Patients

This retrospective study was approved by the local Institutional Ethics Committee (IRB No. 2021148) and the requirement for informed consent was waived. Patients with pathologically confirmed ENKTCL between May 2014 and January 2022 were retrospectively included. Inclusion criteria were the following: 1) no prior tumor-related treatment, 2) PET/CT examination performed before initial treatment, 3) complete clinical data and follow-up information, 4) local radiotherapy or combination with non-anthracycline-based chemotherapy used in subsequent treatment. Exclusion criteria included the following: 1) tumors combined with other malignancies or hematological diseases, 2) poor image quality that could not be evaluated. A total of 126 patients with the required clinical, imaging, and follow-up data were included in the study. These patients were then randomly divided into the training (n = 88) and validation (n = 38) cohorts at a ratio of 7:3. The training cohort included 51 male and 37 female with a median age of 46 years (range: 20–87 years). The validation cohort included 28 male and 10 female with a median age of 47 years (range: 21–71 years).

Clinical Information Collection and Follow-Up

Basic clinical data including sex, age, B symptoms, Ann Arbor stage, lactate dehydrogenase (LDH) levels, β2-microglobulin (β2-MG) levels, Eastern Cooperative Oncology Group (ECOG) performance status score, International Prognostic Index (IPI) score, and radiotherapy were collected. Patients were followed every three months for the first two years and every six months thereafter. Follow-up results were collected through the electronic medical record system or by telephone. The endpoints of this study were progression-free survival (PFS) and OS. PFS was measured in months as the time interval from the date of diagnosis to the first occurrence of disease progression, recurrence, or death as events. OS was measured in months as the time interval from the date of diagnosis to the date of death. At the date of the last follow-up visit, patients who did not experience any events were censored.

PET/CT Image Acquisition

All patients underwent PET/CT whole-body scanning two weeks before treatment. The scanner and tracer were Discovery VCT PET/CT (GE Healthcare, Waukesha, WI, USA) and ^{18}F-FDG, respectively; the radiochemical purity was > 95%. Patients

https://doi.org/10.3348/kjr.2023.0618

Korean Journal of Radiology
KJR

were prohibited from strenuous exercise within 24 hours before examination and fasted for at least 6 hours to ensure their blood glucose level was < 11.1 mmol/L. After quiet rest for 60 ± 10 minutes, 5.5 MBq/kg FDG was injected intravenously, and the scan was performed. The scanning range was from the skull base to the lower femur. CT scanning parameters were as follows: tube voltage, 120 kVp; tube current, 110 mA; and slice thickness, 3.75 mm. The emission scan was acquired for 2 minutes per bed position. Images of four to six bed positions were acquired for each patient, and PET images were reconstructed using an ordered subset expectation maximization algorithm.

Metabolic Parameter Acquisition and Feature Extraction

All images were analyzed by two experienced radiologists who were blinded to the clinical and pathological information. The post-processing workstation (GE Healthcare) was used to semi-automatically segment the three-dimensional volumes of interest (VOIs) of the lesions and calculate MTV and TLG with the threshold of 41% of SUVmax according to the recommendation of the European Association of Nuclear Medicine. Differences of opinion were resolved through discussion. The CT images were segmented using PET images as a reference. Another senior radiologist with 10 years of experience then verified the segmentation to identify any discrepancies. Inconsistencies in the depiction of lesions were rectified. When disagreement arose, the final segmentation results were determined by a more senior radiologist. The open-source software PyRadiomics 3.0.1 (http://github.com/Radiomics/pyradiomics) was used to feature extract and analyze the VOIs segmented by PET and CT sequences. The images were preprocessed by normalization and resampling. The original images were transformed by filters before features extraction: 1) first-order statistical features, 2) shape features, 3) texture features, including gray-level co-occurrence matrix (GLCM), gray-level dependence matrix (GLDM), gray-level run length matrix (GLRLM), gray-level size zone matrix (GLSZM) and neighboring gray-tone difference matrix (NGTDM), 4) high-level features, which extracted features from filtered images.

Feature Selection

To avoid model overfitting, radiomic features associated with survival were first selected by univariable and multivariable Cox regression ($P < 0.05$). Then Z-score normalization was used to reduce the dimensional difference of the remaining features. The variance threshold method and chi-square test ($P < 0.05$) were used to delete the features with low relevance to survival. The least absolute shrinkage and selection operation (LASSO) Cox regression algorithm was applied for dimension reduction, and the optimal parameter Alpha value was obtained using 10-fold cross-validation in the training cohort. Finally, based on the selected non-zero coefficient features, the radiomics score of PFS (RadPFS) and the radiomics score of OS (RadOS) were calculated for each patient according to the linear combination of their respective coefficient weights. The

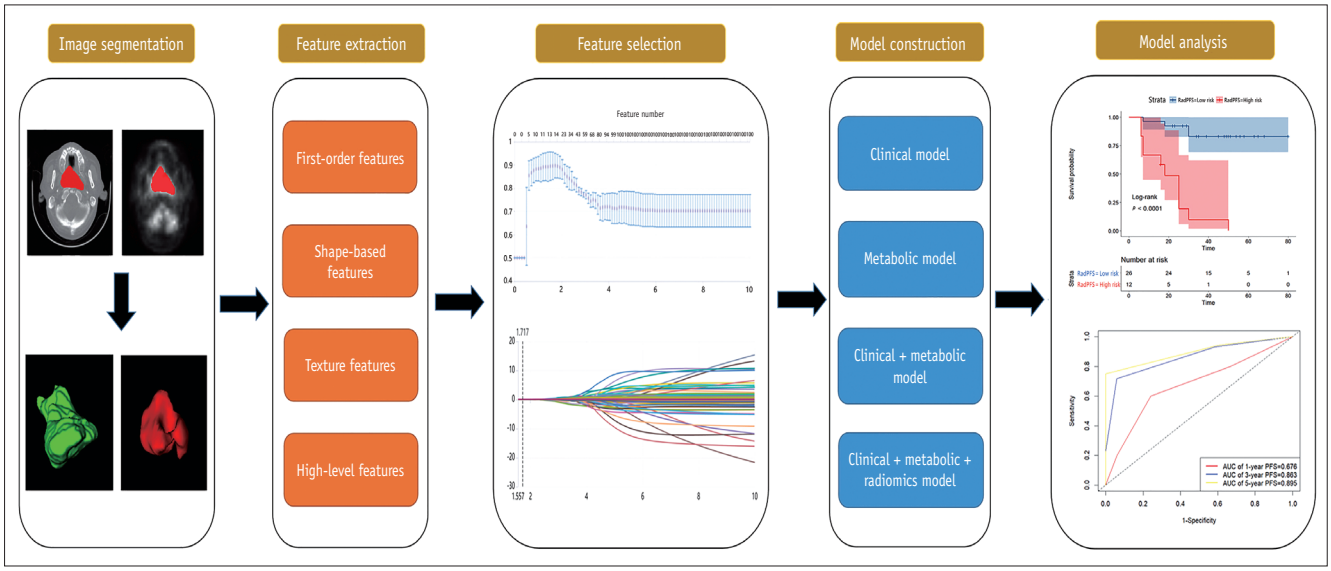

Fig. 1. Workflow of the study. RadPFS = radiomics score of PFS, AUC = area under the curve, PFS = progression-free survival

https://doi.org/10.3348/kjr.2023.0618

analysis framework of this study is shown in Figure 1.

Statistical Analysis

SPSS 26.0 (IBM Corp., Armonk, NY, USA) and R4.2.2 (R Foundation for Statistical Computing, Vienna, Austria) software were used for statistical analysis. X-tile 3.6.1 (RobertL Camp, Yale University, New Haven, CT, USA) software was used to convert continuous variables, including the radiomics scores, into categorical variables and to stratify patients by risk based on optimal cutoff points [18,19]. Categorical variables were compared by Chi-square test. In the training cohort, patients were divided into high-risk and low-risk groups according to the best cut-off values of RadPFS and RadOS, respectively. Kaplan–Meier analysis and Log-rank test were used to compare the survival differences between the two groups and then verified in the validation cohort. Variables with $P < 0.05$ in univariable Cox proportional hazard regression analysis were sequentially entered into multivariable Cox regression analysis to identify independent risk factors related to survival and construct prognostic models. Harrell's C-index was used to evaluate the discriminative ability of each model, ranging from 0.5 to 1, with values closer to 1 indicating better performance. The predictive performance of each model for PFS and OS at 1-, 3-, and 5-year follow-up time points were evaluated using time-dependent receiver operating characteristic (ROC) curves. Statistics with $P < 0.05$ were considered significant.

RESULTS

Clinical Data

Table 1 summarizes the basic clinical information of the training and validation cohorts. No statistically significant differences existed in the clinical data between the two cohorts (all $P > 0.05$). The median PFS and OS were 30 (range: 3–80 months) and 42 (range: 5–88 months) months, respectively. At the final follow-up, 56 (44.4%) patients had relapsed or progressed, and 36 (28.6%) patients had died.

Construction of Radiomics Model

A total of 2264 features were extracted from PET and CT images, respectively. LASSO Cox regression analysis was employed to reduce the dimensionality of features and obtain the optimal parameter Alpha value. Finally, five PET and eight CT features that displayed strong correlations with PFS, as well as two PET features and two CT features that strongly correlated with OS, were selected (Supplementary Tables 1, 2). In Figure 2, the Kaplan–Meier survival curves showed remarkable differences in PFS and OS between high-risk and low-risk groups in both the training and validation cohorts, as determined by the log-rank test (all $P < 0.05$).

Table 1. Baseline clinical characteristics of the patients

Characteristic	Overall cohort (n = 126)	Training cohort (n = 88)	Validation cohort (n = 38)	P*
Sex				0.094
Male	79 (62.7)	51 (58.0)	28 (73.7)	
Female	47 (37.3)	37 (42.0)	10 (26.3)	
Age, yr				0.713
≤ 60	90 (71.4)	62 (70.5)	28 (73.7)	
> 60	36 (28.6)	26 (29.5)	10 (26.3)	
Ann Arbor stage				0.515
I–II	88 (69.8)	63 (71.6)	25 (65.8)	
III–IV	38 (30.2)	25 (28.4)	13 (34.2)	
IPI score				0.415
0–1	66 (52.4)	44 (50.0)	22 (57.9)	
≥ 2	60 (47.6)	44 (50.0)	16 (42.1)	
ECOG score				0.421
0–1	97 (77.0)	66 (75.0)	31 (81.6)	
≥ 2	29 (23.0)	22 (25.0)	7 (18.4)	
LDH, U/L				0.673
≤ 250	83 (65.9)	59 (67.0)	24 (63.2)	
> 250	43 (34.1)	29 (33.0)	14 (36.8)	
β2-MG, mg/L				0.435
≤ 2	53 (42.1)	39 (44.3)	14 (36.8)	
> 2	73 (57.9)	49 (55.7)	24 (63.2)	
B symptom				0.480
Presence	57 (45.2)	38 (43.2)	19 (50.0)	
Absence	69 (54.8)	50 (56.8)	19 (50.0)	
Radiotherapy				0.498
Presence	41 (32.5)	27 (30.7)	14 (36.8)	
Absence	85 (67.5)	61 (69.3)	24 (63.2)	

*For comparing training and validations cohorts.
IPI = International Prognostic Index, ECOG = Eastern Cooperative Oncology Group, LDH = lactate dehydrogenase, β2-MG = β2-microglobulin

Cox Proportional Hazards Analysis

For PFS, in univariable Cox regression analysis, the presence of B symptoms, Ann Arbor stage III–IV, elevated LDH, elevated β2-MG, IPI score ≥ 2, ECOG score ≥ 2; higher SUVmax, MTV, TLG, and RadPFS values; and absence of radiotherapy were adverse factors associated with PFS (all $P < 0.05$). Multivariable analysis (Supplementary Table 3) showed that Ann Arbor stage III–IV (adjusted hazard ratio [HR]: 2.297; 95% confidence interval [CI]: 1.145–4.610;

https://doi.org/10.3348/kjr.2023.0618

Korean Journal of Radiology
KJR

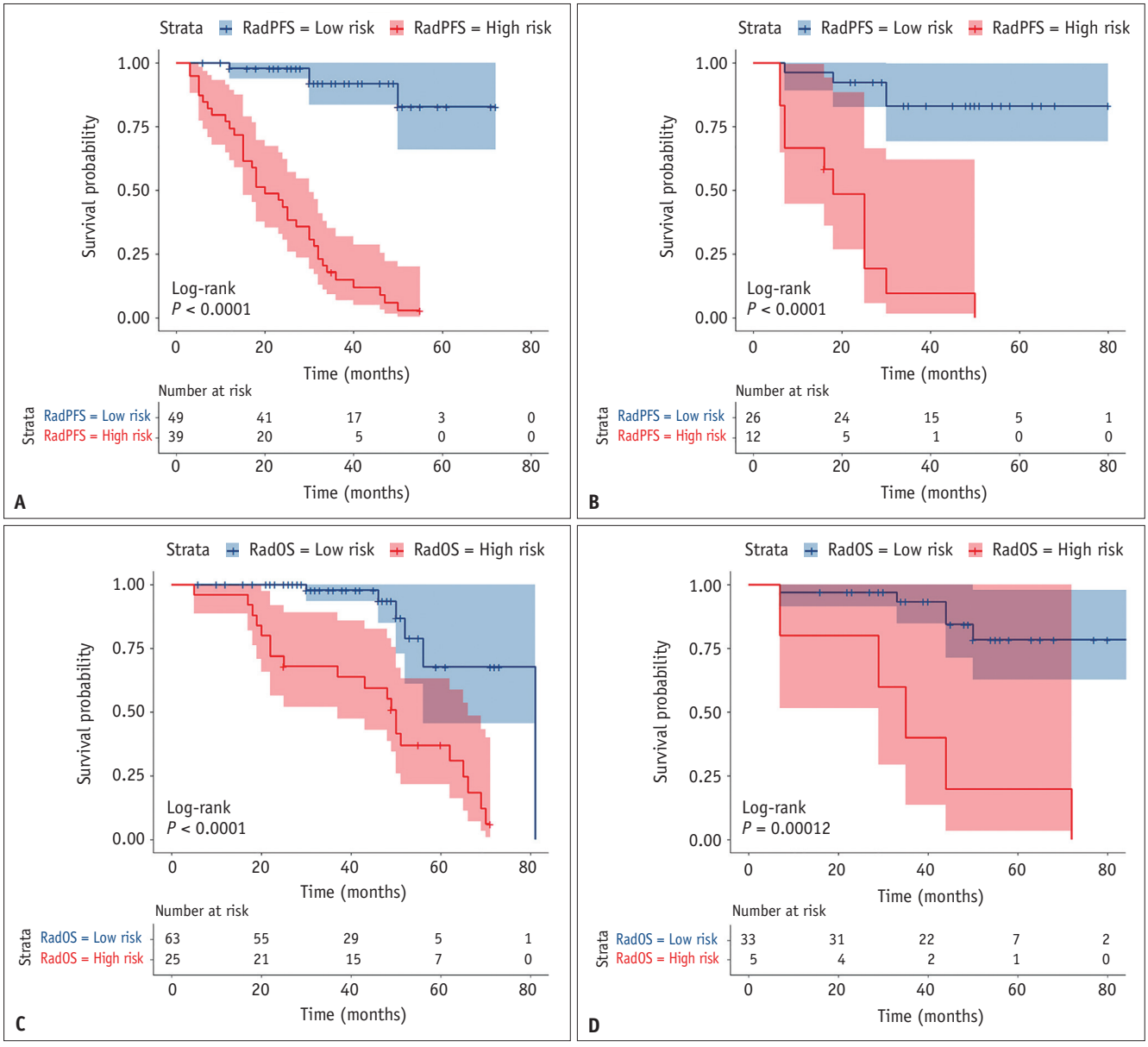

Fig. 2. Kaplan–Meier survival curves of ENKTCL patients as predicted by radiomics scores for PFS **(A, B)** and OS **(C, D)**. The horizontal axis, vertical axis, blue curve, and red curve represent survival time, survival probability, low-risk group, and high-risk group, respectively. **A, C:** Training cohort. **B, D:** Validation cohort. ENKTCL = extranodal nasal-type NK/T cell lymphoma, PFS = progression-free survival, OS = overall survival, RadPFS = radiomics score of PFS, RadOS = radiomics score of OS

P = 0.019), higher SUVmax (adjusted HR: 2.438; 95% CI: 1.096–5.422; *P* = 0.029), and higher RadPFS (adjusted HR: 8.182; 95% CI: 3.248–20.615; *P* < 0.001) values were independent prognostic factors for PFS. Clinical (Ann Arbor stage), metabolic (SUVmax), clinical + metabolic (Ann Arbor stage + SUVmax), and clinical + metabolic + radiomics (Ann Arbor stage + SUVmax + RadPFS) models were constructed based on the results.

For OS, in univariable Cox regression analysis, the presence of B symptoms, Ann Arbor stage III–IV, elevated β2-MG, IPI score ≥ 2, and ECOG score ≥ 2, and higher SUVmax, MTV, TLG, and RadOS values were significantly associated with worse OS (all *P* < 0.05). Multivariable analysis (Supplementary Table 4) showed that elevated β2-MG (adjusted HR: 5.001; 95% CI: 1.114–22.447; *P* = 0.036), ECOG score ≥ 2 (adjusted HR: 2.762; 95% CI: 1.089–7.002; *P* = 0.032), higher SUVmax (adjusted HR: 3.436; 95% CI: 1.008–11.715; *P* = 0.049), and RadOS (adjusted HR: 2.821; 95% CI: 1.011–7.870; *P* = 0.048) values were independent prognostic factors for OS. Clinical (β2-MG +

https://doi.org/10.3348/kjr.2023.0618

ECOG score), metabolic (SUVmax), clinical + metabolic (β2-MG + ECOG score + SUVmax), and clinical + metabolic + radiomics (β2-MG + ECOG score + SUVmax + RadOS) models were constructed based on the above results.

Performance and Validation of Prognostic Models

The clinical + metabolic + radiomics model had the best predictive performance in both the training (C-index for PFS: 0.865, 95% CI: 0.821–0.908; C-index for OS: 0.876, 95% CI: 0.818–0.935) and validation (C-index for PFS: 0.805, 95% CI: 0.680–0.931; C-index for OS: 0.833, 95% CI: 0.725–0.942) cohorts (Table 2).

In predicting PFS at 1-, 3-, and 5-year clinical follow-ups, the clinical + metabolic + radiomics model consistently outperformed other models. Specifically, for the one-year follow-up among the training cohort, the area under the curve (AUC) values were as follows: clinical + metabolic + radiomics model (0.857), clinical model (0.652), metabolic model (0.771), and clinical + metabolic model (0.804). Similar patterns were observed for the 3-, and 5-year follow-ups. For the validation cohort, at one-year follow-up, the AUC values were 0.676, 0.533, 0.503, and 0.518 for the clinical + metabolic + radiomics, clinical, metabolic, and clinical + metabolic models, respectively. Again, the 3-, and 5-year follow-ups reflected the same trend. The time-dependent ROC curves are provided in the Supplementary Material (Supplementary Fig. 1).

Furthermore, when predicting the survival risk for OS at 1-, 3-, and 5-years, the clinical + metabolic + radiomics model demonstrated improved predictive performance compared to other models (clinical + metabolic + radiomics model vs. clinical model vs. metabolic model vs. clinical + metabolic model), the AUC values for the training cohort were 0.933, 0.902, 0.646, and 0.909 for 1 year; 0.851, 0.767, 0.645, and 0.803 for 3 years; and 0.853, 0.827, 0.636, and 0.896 for 5 years, respectively. In the validation cohort, the AUC values were 0.819, 0.597, 0.750, and 0.750 for 1 year; 0.803, 0.574, 0.780, and 0.738 for 3 years; and 0.785, 0.640, 0.690, and 0.758 for 5 years, respectively. The time-dependent ROC curves are provided in the Supplement material (Supplementary Fig. 2).

DISCUSSION

This study preliminarily explored the prognostic value of baseline PET/CT radiomics features combined with clinical indicators and metabolic parameters in patients with ENKTCL. The results revealed that the clinical + metabolic + radiomics model had the highest AUC values for predicting PFS and OS in both the training and validation cohorts. The clinical + metabolic + radiomics model better predicted the prognosis of ENKTCL patients and contributed to more effective treatment implementation by clinicians.

The multivariable Cox analysis conducted in this study showed that the Ann Arbor stage, β2-MG level, and ECOG score were associated with the prognosis of ENKTCL patients, which was roughly consistent with previous findings [20,21]. Ann Arbor staging is a standard method widely used in lymphoma staging, with a higher stage indicating a more widespread disease, faster progression, and poorer

Table 2. Harrell's C-index results of each model in the training cohort and the validation cohort

Models	Training cohort		Validation cohort	
	C-index	95% CI	C-index	95% CI
PFS				
Clinical model	0.678	0.604–0.752	0.605	0.473–0.737
Metabolic model	0.701	0.638–0.764	0.597	0.461–0.734
Clinical + metabolic model	0.781	0.722–0.840	0.652	0.504–0.800
Radiomics score (RadPFS)	0.791	0.735–0.847	0.788	0.691–0.885
Clinical + metabolic + radiomics model	0.865	0.821–0.908	0.805	0.680–0.931
OS				
Clinical model	0.832	0.761–0.904	0.564	0.403–0.725
Metabolic model	0.640	0.587–0.693	0.737	0.633–0.841
Clinical + metabolic model	0.854	0.791–0.916	0.788	0.676–0.901
Radiomics score (RadOS)	0.769	0.680–0.858	0.705	0.549–0.861
Clinical + metabolic + radiomics model	0.876	0.818–0.935	0.833	0.725–0.942

CI = confidence interval, PFS = progression-free survival, RadPFS = radiomics score of PFS, OS = overall survival, RadOS = radiomics score of OS

https://doi.org/10.3348/kjr.2023.0618

Korean Journal of Radiology
KJR

prognosis [22]. Meanwhile, β2-MG—a component of major histocompatibility complex class I molecules—is associated with the prognosis of lymphoproliferative diseases and has been included in the risk stratification system for various disorders [23,24]. According to Prizment et al. [25], β2-MG is linked to tumor load and cell turnover, influencing tumor growth, survival, and apoptosis. ECOG score is a widely used indicator of patient physical ability and daily activity, wherein higher scores suggest poor physical fitness, reduced treatment tolerance, and an unfavorable prognosis [26]. Clinical models were established in this study using the above risk factors to predict both PFS and OS. However, the clinical models underperformed in the validation cohort, indicating limited predictive value. This may be attributed to the lack of specificity in the clinical manifestations of ENKTCL patients. Further, the relatively insufficient information from the clinical metrics was inapplicable for further prognosis prediction. Therefore, including more metrics like metabolism and radiomics will aid in more precise risk stratification.

A battery of ENKTCL prognostic models have been proposed and widely employed in clinical practice [27,28]. Despite improving the risk stratification of patients and having some predictive prognostic value, these models have limited sensitivity and do not include individualized information or imaging [29,30]. Imaging features are critical for assessing tumor biology and microenvironment. ^{18}F-FDG PET/CT has been extensively utilized in the clinical management of lymphoma as it can reveal concealed lesions, comprehensively evaluate the extent of lesion involvement, and infer the metabolic activity and proliferation status of the lesion [31]. This study reported that SUVmax is an independent risk factor for predicting both PFS and OS, this is consistent with the findings of Bai et al. [32], who reported that higher SUVmax values showed considerably greater chances of treatment failure. Higher SUVmax values indicate more active tumor cell metabolism and faster proliferation rate linked to adverse biological behaviors such as tumor size and local invasion. Nonetheless, other studies have reported inconsistent results and argued that SUVmax might not provide valuable information for prognosis prediction [33,34]. This inconsistency may be due to the heterogeneity of enrolled patients and SUVmax only being able to measure the maximum standard uptake value of tumor lesions instead of the overall tumor metabolic load. New evaluation schemes should be proposed, including individualized metrics to enhance prediction.

Radiomics can extract biological behavior information to reflect the intrinsic properties of lesions for predicting tumor heterogeneity, progression, and prognosis. In this study, RadPFS and RadOS derived from radiomics features extracted from PET/CT images can effectively identify high-risk and low-risk patients with ENKTCL ($P < 0.05$). Currently, few studies have used radiomics to predict the prognosis of ENKTCL. Ko et al. [35] retrospectively analyzed the baseline PET images of 17 ENKTCL patients and found that texture features were independent predictors of disease progression and could improve patient prognosis stratification. Wang et al. [36] reported that the PET-based radiomics model had inferior predictive capabilities for PFS and OS in ENKTCL patients relative to metabolic models. This study simultaneously extracted radiomics features from CT and PET images for further prediction. The CT features cover the deficiency of PET in morphological and structural information. The optimal radiomics features extracted in this study mainly consist of shape and texture features including GLCM, GLDM, GLSZM, and GLRLM. The shape features primarily include the least axis length and maximum 2D diameter, which describe the length of the spatially shortest axis of the lesion and the diameter of the maximum cross-section of the lesion, respectively [37]. Larger values indicate a malignancy trend of the lesion and an increased risk of metastasis and recurrence. GLCM reflects the gray relationship between two voxels in a certain direction and distance, representing the spatial correlation of gray values in the image [38]. GLDM measures grayscale similarity and dependence, while GLSZM evaluates texture uniformity [39,40]. GLRLM mainly reflects the roughness and directionality of the texture [41]. Changes in these texture features reflect the detailed structure of lymphomas, which are related to the degree of malignancy, heterogeneity, and treatment response of patients. Radiomics can quantify image information from multiple perspectives and help improve the predictive performance of clinical + metabolic + radiomics models.

This study had the following limitations. First, it is a retrospective single-center study with a small sample size, and the efficacy of the model needs to be further verified with extended research. Second, the study did not include multimodal information such as genes and proteins, which warrant further analysis. Third, this study utilized the radiomics analysis method, which can be combined with deep learning techniques in the future, such as convolutional neural networks, to optimize model performance.

 https://doi.org/10.3348/kjr.2023.0618

In conclusion, the model constructed with the combination of PET/CT radiomics features, clinical information, and metabolic parameters can accurately and noninvasively predict the prognosis of ENKTCL patients. Utilizing this approach has the potential to provide a crucial reference for subsequent treatment and follow-up.

Supplement

The Supplement is available with this article at https://doi.org/10.3348/kjr.2023.0618.

Availability of Data and Material

The datasets generated or analyzed during the study are available from the corresponding author on reasonable request.

Conflicts of Interest

The authors have no potential conflicts of interest to disclose.

Author Contributions

Conceptualization: Meiyun Wang, Yan Bai, Yu Luo. Data curation: Yu Luo, Zhun Huang, Zihan Gao, Bingbing Wang, Qingxia Wu. Formal analysis: Yu Luo, Zhun Huang. Funding acquisition: Meiyun Wang. Investigation: Yu Luo, Zihan Gao, Bingbing Wang. Methodology: Yu Luo, Zhun Huang, Yanwei Zhang, Yan Bai, Qingxia Wu. Project administration: Meiyun Wang. Resources: Meiyun Wang, Yan Bai. Software: Yu Luo, Zihan Gao, Yanwei Zhang, Qingxia Wu. Supervision: Yu Luo, Yanwei Zhang. Validation: Yu Luo, Zihan Gao, Bingbing Wang. Visualization: Yanwei Zhang, Yan Bai. Writing—original draft: Yu Luo. Writing—review & editing: all authors.

ORCID IDs

Yu Luo
https://orcid.org/0000-0002-8379-4461
Zhun Huang
https://orcid.org/0000-0002-9483-0528
Zihan Gao
https://orcid.org/0009-0007-0276-0539
Bingbing Wang
https://orcid.org/0009-0004-4578-7895
Yanwei Zhang
https://orcid.org/0000-0003-1806-6617
Yan Bai
https://orcid.org/0000-0003-2421-4129
Qingxia Wu
https://orcid.org/0000-0001-6214-8033
Meiyun Wang
https://orcid.org/0000-0002-7163-2617

Funding Statement

This study was funded by the Medical Science and Technology Research Project of Henan Province (SBGJ202101002).

REFERENCES

1. Han L, Liu F, Li R, Li Z, Chen X, Zhou Z, et al. Role of programmed death ligands in effective T-cell interactions in extranodal natural killer/T-cell lymphoma. *Oncol Lett* 2014;8:1461-1469
2. Ryu KJ, Lee JY, Choi ME, Yoon SE, Cho J, Ko YH, et al. Serum-derived exosomal MicroRNA profiles can predict poor survival outcomes in patients with extranodal natural killer/T-cell lymphoma. *Cancers (Basel)* 2020;12:3548
3. Peng YY, Xiong YY, Zhang LX, Wang J, Zhang HB, Xiao Q, et al. Allogeneic hematopoietic stem cell transplantation in extranodal natural killer/T-cell lymphoma. *Turk J Haematol* 2021;38:126-137
4. Fox CP, Civallero M, Ko YH, Manni M, Skrypets T, Pileri S, et al. Survival outcomes of patients with extranodal natural-killer T-cell lymphoma: a prospective cohort study from the international T-cell project. *Lancet Haematol* 2020;7:e284-e294
5. Wang L, Wang H, Wang JH, Xia ZJ, Lu Y, Huang HQ, et al. Post-treatment plasma EBV-DNA positivity predicts early relapse and poor prognosis for patients with extranodal NK/T cell lymphoma in the era of asparaginase. *Oncotarget* 2015;6:30317-30326
6. Li H, Shao G, Zhang Y, Chen X, Du C, Wang K, et al. Nomograms based on SUVmax of 18F-FDG PET/CT and clinical parameters for predicting progression-free and overall survival in patients with newly diagnosed extranodal natural killer/T-cell lymphoma. *Cancer Imaging* 2021;21:9
7. Wang H, Shen G, Jiang C, Li L, Cui F, Tian R. Prognostic value of baseline, interim and end-of-treatment 18F-FDG PET/CT parameters in extranodal natural killer/T-cell lymphoma: a meta-analysis. *PLoS One* 2018;13:e0194435
8. Chang Y, Fu X, Sun Z, Xie X, Wang R, Li Z, et al. Utility of baseline, interim and end-of-treatment 18F-FDG PET/CT in extranodal natural killer/T-cell lymphoma patients treated with L-asparaginase/pegaspargase. *Sci Rep* 2017;7:41057
9. Kim CY, Hong CM, Kim DH, Son SH, Jeong SY, Lee SW, et al. Prognostic value of whole-body metabolic tumour volume and total lesion glycolysis measured on 18F-FDG PET/CT in patients with extranodal NK/T-cell lymphoma. *Eur J Nucl Med*

Mol Imaging 2013;40:1321-1329
10. Guidetti A, Dodero A, Lorenzoni A, Pizzamiglio S, Argiroffi G, Chiappella A, et al. Combination of Deauville score and quantitative positron emission tomography parameters as a predictive tool of anti-CD19 chimeric antigen receptor T-cell efficacy. *Cancer* 2023;129:255-263
11. Hinzpeter R, Mirshahvalad SA, Kulanthaivelu R, Ortega C, Metser U, Liu ZA, et al. Prognostic value of [18F]-FDG PET/CT radiomics combined with sarcopenia status among patients with advanced gastroesophageal cancer. *Cancers (Basel)* 2022;14:5314
12. Zheng X, He B, Hu Y, Ren M, Chen Z, Zhang Z, et al. Diagnostic accuracy of deep learning and radiomics in lung cancer staging: a systematic review and meta-analysis. *Front Public Health* 2022;10:938113
13. Wu L, Zhao Y, Lin P, Qin H, Liu Y, Wan D, et al. Preoperative ultrasound radiomics analysis for expression of multiple molecular biomarkers in mass type of breast ductal carcinoma in situ. *BMC Med Imaging* 2021;21:84
14. Lue KH, Huang CH, Hsieh TC, Liu SH, Wu YF, Chen YH. Systemic inflammation index and tumor glycolytic heterogeneity help risk stratify patients with advanced epidermal growth factor receptor-mutated lung adenocarcinoma treated with tyrosine kinase inhibitor therapy. *Cancers (Basel)* 2022;14:309
15. Li Y, Zhang Y, Fang Q, Zhang X, Hou P, Wu H, et al. Radiomics analysis of [18F]FDG PET/CT for microvascular invasion and prognosis prediction in very-early- and early-stage hepatocellular carcinoma. *Eur J Nucl Med Mol Imaging* 2021;48:2599-2614
16. Kirienko M, Sollini M, Corbetta M, Voulaz E, Gozzi N, Interlenghi M, et al. Radiomics and gene expression profile to characterise the disease and predict outcome in patients with lung cancer. *Eur J Nucl Med Mol Imaging* 2021;48:3643-3655
17. Peng H, Dong D, Fang MJ, Li L, Tang LL, Chen L, et al. Prognostic value of deep learning PET/CT-based radiomics: potential role for future individual induction chemotherapy in advanced nasopharyngeal carcinoma. *Clin Cancer Res* 2019;25:4271-4279
18. Guo H, Li B, Diao L, Wang H, Chen P, Jiang M, et al. An immune-based risk-stratification system for predicting prognosis in pulmonary sarcomatoid carcinoma (PSC). *Oncoimmunology* 2021;10:1947665
19. Camp RL, Dolled-Filhart M, Rimm DL. X-tile: a new bio-informatics tool for biomarker assessment and outcome-based cut-point optimization. *Clin Cancer Res* 2004;10:7252-7259
20. Parvez A, Tau N, Hussey D, Maganti M, Metser U. 18F-FDG PET/CT metabolic tumor parameters and radiomics features in aggressive non-Hodgkin's lymphoma as predictors of treatment outcome and survival. *Ann Nucl Med* 2018;32:410-416
21. Wu W, Ren K, Chen X, Li N, Zhou H, Jiang M, et al. A controlling nutritional status score is an independent predictor for patients with newly diagnosed nasal-type extranodal NK/T-cell lymphoma based on asparaginase-containing regimens. *Cancer Med* 2023;12:9439-9448
22. McGrath LA, Ryan DA, Warrier SK, Coupland SE, Glasson WJ. Conjunctival lymphoma. *Eye (Lond)* 2023;37:837-848
23. Kang S, Cho H, Kim S, Lee K, Kang EH, Park JS, et al. A new prognostic index for extranodal natural killer/T-cell lymphoma: incorporation of serum β-2 microglobulin to PINK. *Cancer Res Treat* 2023;55:314-324
24. Kim HD, Cho H, Kim S, Lee K, Kang EH, Park JS, et al. Prognostic stratification of patients with Burkitt lymphoma using serum β2-microglobulin levels. *Cancer Res Treat* 2021;53:847-856
25. Prizment AE, Linabery AM, Lutsey PL, Selvin E, Nelson HH, Folsom AR, et al. Circulating beta-2 microglobulin and risk of cancer: the atherosclerosis risk in communities study (ARIC). *Cancer Epidemiol Biomarkers Prev* 2016;25:657-664
26. Semere W, Althouse AD, Rosland AM, White D, Arnold R, Chu E, et al. Poor patient health is associated with higher caregiver burden for older adults with advanced cancer. *J Geriatr Oncol* 2021;12:771-778
27. Wang H, Fu BB, Gale RP, Liang Y. NK-/T-cell lymphomas. *Leukemia* 2021;35:2460-2468
28. Chen SY, Yang Y, Qi SN, Wang Y, Hu C, He X, et al. Validation of nomogram-revised risk index and comparison with other models for extranodal nasal-type NK/T-cell lymphoma in the modern chemotherapy era: indication for prognostication and clinical decision-making. *Leukemia* 2021;35:130-142
29. Huang JJ, Zhu YJ, Xia Y, Zhao W, Lin TY, Jiang WQ, et al. A novel prognostic model for extranodal natural killer/T-cell lymphoma. *Med Oncol* 2012;29:2183-2190
30. Suzuki R, Suzumiya J, Yamaguchi M, Nakamura S, Kameoka J, Kojima H, et al. Prognostic factors for mature natural killer (NK) cell neoplasms: aggressive NK cell leukemia and extranodal NK cell lymphoma, nasal type. *Ann Oncol* 2010;21:1032-1040
31. Oñate-Ocaña LF, Cortés V, Castillo-Llanos R, Terrazas A, Garcia-Perez O, Pitalúa-Cortes Q, et al. Metabolic tumor volume changes assessed by interval 18fluorodeoxyglucose positron emission tomography-computed tomography for the prediction of complete response and survival in patients with diffuse large B-cell lymphoma. *Oncol Lett* 2018;16:1411-1418
32. Bai B, Huang HQ, Cai QC, Fan W, Wang XX, Zhang X, et al. Predictive value of pretreatment positron emission tomography/computed tomography in patients with newly diagnosed extranodal natural killer/T-cell lymphoma. *Med Oncol* 2013;30:339
33. Guo R, Xu P, Xu H, Miao Y, Li B. The predictive value of pre-treatment 18F-FDG PET/CT on treatment outcome in early-stage extranodal natural killer/T-cell lymphoma. *Leuk Lymphoma* 2020;61:2659-2664
34. Khong PL, Huang B, Lee EY, Chan WK, Kwong YL. Midtreatment 18F-FDG PET/CT scan for early response assessment of SMILE therapy in natural killer/T-cell lymphoma: a prospective study from a single center. *J Nucl Med* 2014;55:911-916
35. Ko KY, Liu CJ, Ko CL, Yen RF. Intratumoral heterogeneity of pretreatment 18F-FDG PET images predict disease progression in patients with nasal type extranodal natural killer/T-cell

lymphoma. *Clin Nucl Med* 2016;41:922-926
36. Wang H, Zhao S, Li L, Tian R. Development and validation of an 18F-FDG PET radiomic model for prognosis prediction in patients with nasal-type extranodal natural killer/T cell lymphoma. *Eur Radiol* 2020;30:5578-5587
37. Zhai TT, Langendijk JA, van Dijk LV, van der Schaaf A, Sommers L, Vemer-van den Hoek JGM, et al. Pre-treatment radiomic features predict individual lymph node failure for head and neck cancer patients. *Radiother Oncol* 2020;146:58-65
38. Peng Z, Wang Y, Wang Y, Jiang S, Fan R, Zhang H, et al. Application of radiomics and machine learning in head and neck cancers. *Int J Biol Sci* 2021;17:475-486
39. An P, Lin Y, Hu Y, Qin P, Ye Y, Gu W, et al. Predicting model of biochemical recurrence of prostate carcinoma (PCa-BCR) using MR perfusion-weighted imaging-based radiomics. *Technol Cancer Res Treat* 2023;22:15330338231166766
40. Yu Q, Liu J, Lin H, Lei P, Fan B. Application of radiomics model of CT images in the identification of ureteral calculus and phlebolith. *Int J Clin Pract* 2022;2022:5478908
41. Yang H, Wang L, Shao G, Dong B, Wang F, Wei Y, et al. A combined predictive model based on radiomics features and clinical factors for disease progression in early-stage non-small cell lung cancer treated with stereotactic ablative radiotherapy. *Front Oncol* 2022;12:967360

https://doi.org/10.3348/kjr.2023.0618